A minimal model of insulin secretion and kinetics to assess hepatic insulin extraction

Gianna Toffolo, Marco Campioni, Rita Basu, Robert A. Rizza and Claudio Cobelli

Am J Physiol Endocrinol Metab 290:169-176, 2006. First published Sep 6, 2005;
doi:10.1152/ajpendo.00473.2004

AJP - Endocrinology and Metabolism publishes results of original studies about endocrine and metabolic systems on any level of organization. It is published 12 times a year (monthly) by the American Physiological Society, 9650 Rockville Pike, Bethesda MD 20814-3991. ISSN: 0193-1849, ESSN: 1522-1555. Visit our website at http://www.the-aps.org/.

Am J Physiol Endocrinol Metab 290: E169–E176, 2006.
First published September 6, 2005; doi:10.1152/ajpendo.00473.2004.

A minimal model of insulin secretion and kinetics to assess hepatic insulin extraction

Gianna Toffolo,[1] Marco Campioni,[1] Rita Basu,[2] Robert A. Rizza,[2] and Claudio Cobelli[1]

[1]*Department of Information Engineering, University of Padua, Padua, Italy; and* [2]*Department of Internal Medicine, Division of Endocrinology, Diabetes, Metabolism and Nutrition, Mayo Clinic and Foundation, Rochester, Minnesota*

Submitted 5 October 2004; accepted in final form 30 August 2005

Toffolo, Gianna, Marco Campioni, Rita Basu, Robert A. Rizza, and Claudio Cobelli. A minimal model of insulin secretion and kinetics to assess hepatic insulin extraction *Am J Physiol Endocrinol Metab* 290: E169–E176, 2006. First published September 6, 2005; doi:10.1152/ajpendo.00473.2004.—The liver is the principal site of insulin degradation, and assessing its ability to extract insulin is important to understand several pathological states. Noninvasive quantification of hepatic extraction (HE) in an individual requires comparing the profiles of insulin secretion (ISR) and posthepatic insulin delivery rate (IDR). To do this, we propose here the combined use of the classical C-peptide minimal model with a new minimal model of insulin delivery and kinetics. The models were identified on insulin-modified intravenous glucose tolerance test (IM-IVGTT) data of 20 healthy subjects. C-peptide kinetics were fixed to standard population values, whereas insulin kinetics were assessed in each individual, along with IDR parameters, thanks to the presence of insulin decay data observed after exogenous insulin administration. From the two models, profiles of ISR and IDR were predicted, and ISR and IDR indexes of β-cell responsivity to glucose in the basal state, as well as during first- and second-phase secretion, were estimated. HE profile, obtained by comparing ISR and IDR profiles, showed a rapid suppression immediately after the glucose administration. HE indexes, obtained by comparing ISR and IDR indexes, indicated that the liver is able to extract 70 ± 9% of insulin passing through it in the basal state and 54 ± 14% during IM-IVGTT. In conclusion, insulin secretion, kinetics, and hepatic extraction can be reliably assessed during an IM-IVGTT by using insulin and C-peptide minimal models.

hepatic extraction; intravenous glucose tolerance test; parameter estimation

THE LIVER PLAYS A MAJOR ROLE in determining circulating insulin levels because it is responsible for the elimination of the prevalent fraction of insulin. A quantitative assessment of hepatic insulin extraction (HE) in an individual, in the basal state and/or during a glucose perturbation, is an essential step in deriving an overall parametric picture of the glucose regulatory system. Because a direct measurement requires invasive protocols, with catheters placed in the artery and hepatic vein, indirect approaches based on mathematical models are essential to infer HE from plasma measurements (8). Several approaches have been proposed that combine the assessment of insulin secretion (ISR) from C-peptide data and insulin delivery rate (IDR) in plasma after its first pass through the liver from insulin data to provide HE noninvasively in humans during a glucose perturbation, either intravenously or orally (6, 7, 22, 24). Linking ISR and IDR to plasma measurements of C-peptide and insulin requires a description of C-peptide and insulin kinetics. Different compartmental structures were assumed for insulin (from 1 to 3 compartments) and C-peptide kinetics (1 or 2 compartments), as well as different functional descriptions for insulin secretion/delivery during glucose perturbation. Because all these approaches were aimed at simultaneously estimating kinetics and secretion, assessment of secretion could be biased because of undesired compensations that may arise in parameter estimation of kinetics and secretion processes (20). Moreover, HE was often assumed to be constant during the experiment, even if evidence exists that this process varies in time during a glucose/insulin perturbation (6, 15), e.g., due to saturable receptor-mediated mechanisms (12) and/or dependence of HE from blood flow (22).

The purpose here is to assess HE during an intravenous glucose load in humans by using the minimal-modeling approach. This approach has already been applied to C-peptide data, measured during an intravenous glucose tolerance test (IVGTT) (20) to develop the minimal model of C-peptide secretion and kinetics and then extended to an insulin-modified (IM)-IVGTT; i.e., a bolus or a 5-min square wave of insulin is infused 20 min after the glucose bolus (21). Standard population values were used for C-peptide kinetics (23) to avoid compensation between kinetic and secretion parameters, thus reliably measuring insulin secretion and indexes of β-cell responsivity to glucose. Unfortunately, the extension of this approach to assess insulin delivery rate and kinetics from insulin data is not straightforward, mainly because standard values are not available for insulin kinetics. To solve this problem, we took advantage of the unique features of IM-IVGTT: these data are more informative than standard IVGTT because the decay of insulin concentration observed after the exogenous insulin administration facilitates a reliable estimation of insulin kinetics in each individual, a prerequisite to avoiding errors in modeling secretion. The combined use of insulin and C-peptide minimal models was then explored as a tool to assess HE.

Database. The data originated from a previous study (2), to which we refer for details on experimental protocols and analytical methods. Briefly, 20 normal subjects (16 males and 4 females, mean age 44 ± 5 yr, BMI 26.03 ± 0.68 kg/m^2) underwent an IM-IVGTT that consisted of an intravenous injection of glucose (0.3 g/kg body wt) followed by a square wave (from 20 to 25 min) of insulin infusion (0.02 U/kg body wt). Blood was sampled at 0, 2, 4, 6, 8, 10, 15, 20, 22, 25, 26, 28, 31, 35, 45, 60, 75, 90, 120, 180, and 240 min after the glucose injection, and glucose, C-peptide, and insulin concentrations were measured.

Address for reprint requests and other correspondence: Claudio Cobelli, Dept. of Information Engineering, Via Gradenigo 6a, 35131, Padua, Italy (e-mail: cobelli@dei.unipd.it).

The costs of publication of this article were defrayed in part by the payment of page charges. The article must therefore be hereby marked "*advertisement*" in accordance with 18 U.S.C. Section 1734 solely to indicate this fact.

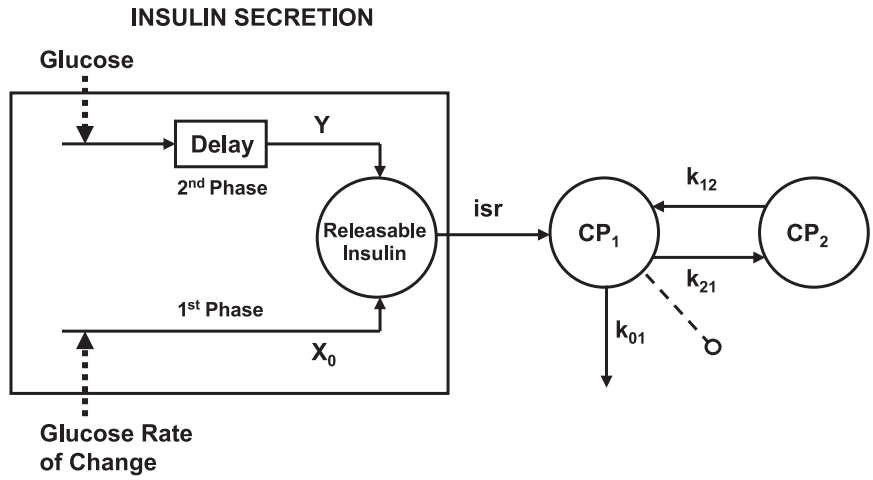

Fig. 1. Minimal model of C-peptide secretion and kinetics. CP_1 and CP_2, C-peptide concentrations above basal in the accessible and peripheral compartments, respectively; k_{01}, k_{21}, and k_{12}, trasfer rate parameters; isr, insulin secretion above basal; Y, provision of new insulin to the β-cells controlled by glucose concentration; X_0, amount of insulin secreted as an impulse during first-phase secretion in response to rapid increase of glucose concentration after glucose bolus.

METHODS

C-peptide model. The minimal model of C-peptide secretion and kinetics that we described earlier (21) was used to assess ISR. C-peptide kinetics are described by the linear two-compartment model (Fig. 1) that was originally proposed by Eaton et al. (7)

$$\begin{aligned} \dot{CP}_1(t) &= -[k_{01}+k_{21}]CP_1(t) + k_{12}CP_2(t) + isr(t) \quad CP_1(0)=0 \\ \dot{CP}_2(t) &= k_{21}CP_1(t) - k_{12}CP_2(t) \quad CP_2(0)=0 \end{aligned} \tag{1}$$

where CP_1 and CP_2 (pmol/l) are C-peptide concentrations (above basal) in the accessible and peripheral compartment respectively, k_{01}, k_{21}, and k_{12} (min^{-1}) are transfer rate parameters, and isr ($pmol \cdot l^{-1} \cdot min^{-1}$) is secretion above basal entering the accessible compartment, normalized by the volume of distribution of *compartment 1*.

It was assumed that isr was proportional to the amount X (pmol/l) of insulin in the β-cells, resulting from the balance between isr and provision Y ($pmol \cdot l^{-1} \cdot min^{-1}$) of new insulin to the β-cells.

$$isr(t) = mX(t) \tag{2}$$

$$\dot{X}(t) = -mX(t) + Y(t) \quad X(0) = X_0 \tag{3}$$

X_0 is responsible for first-phase secretion, whereas the slower second phase derives from provision Y, which is controlled by glucose according to the following equation:

$$\dot{Y}(t) = -\alpha\{Y(t) - \beta[G(t) - h]\} \quad Y(0) = 0 \tag{4}$$

i.e., in response to an elevated glucose level, Y and thus isr tends with a time constant of 1/α (min), toward a steady-state value that is linearly related via parameter β (min^{-1}) to glucose concentration G (mmol/l) above the threshold value *h*.

From model parameters, the ISR profile (pmol/min) was reconstructed as

$$ISR(t) = [k_{01}C_{1b} + isr(t)]V_C = [k_{01}C_{1b} + mX(t)]V_C \tag{5}$$

where V_C is the distribution volume of the accessible compartment, and C_{1b} is the end-test C-peptide concentration.

Indexes of responsivity to glucose of first- and second-phase and basal secretion were also calculated. First-phase responsivity to glucose, Φ_1 (dimensionless), is defined as the ratio between the incremental amount of insulin secreted during the first phase and the maximum increment of plasma glucose concentration ΔG (mmol/l).

$$\Phi_1 = X_0/\Delta G \tag{6}$$

Second-phase responsivity to glucose, Φ_2 (min^{-1}) equals parameter β, which describes the stimulatory effect of glucose concentration on provision

$$\Phi_2 = \beta \tag{7}$$

Finally, basal responsivity to glucose, Φ_b (min^{-1}), is defined as

$$\Phi_b = isr_b/G_b = k_{01}C_{1b}/G_b \tag{8}$$

where G_b is the end-test glucose concentration.

Insulin model. To assess IDR from plasma insulin concentration, a linear single-compartment model was used (Fig. 2):

$$\dot{I}(t) = -nI(t) + idr(t) + U(t)/V_I \quad I(0) = 0 \tag{9}$$

where I (pmol/l) is insulin concentration above basal (end-test) value, *n* (min^{-1}) is the rate constant of insulin disappearance, idr ($pmol \cdot l^{-1} \cdot min^{-1}$) is insulin delivery rate above basal normalized to the volume of distribution, U (pmol/min) is the exogenous insulin input, different from zero in the 20–25-min interval, and V_I (l) is the insulin distribution volume.

For idr, a description similar to that proposed to describe insulin secretion from C-peptide data was adopted

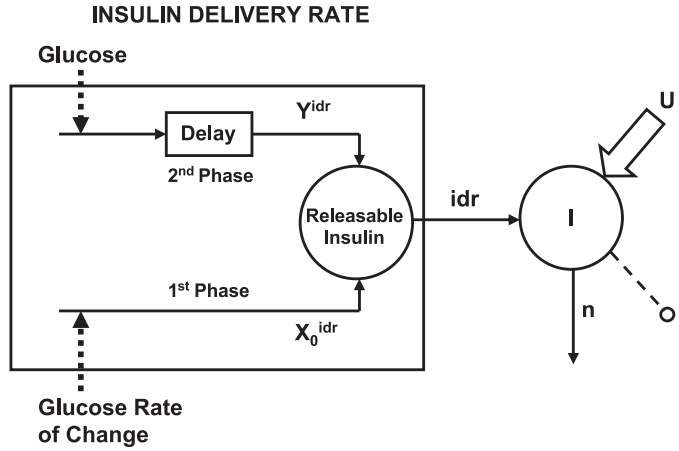

Fig. 2. Minimal model of insulin delivery rate and kinetics. I, plasma insulin concentration above basal, accessible to measurement; *n*, rate constant of insulin disappearance; U, exogenous insulin input; idr, posthepatic insulin delivery rate above basal. Y^{idr} and X_0^{idr} are its parameters, related to provision of new insulin to β-cells and first-phase secretion, respectively.

$$\begin{aligned} idr(t) &= m^{IDR}X^{IDR}(t) \\ \dot{X}^{IDR}(t) &= -m^{IDR}X^{IDR}(t) + Y^{IDR}(t) \quad X^{IDR}(0) = X_0{}^{IDR} \\ \dot{Y}^{IDR}(t) &= -\alpha^{IDR}\{Y^{IDR}(t) - \beta^{IDR}[G(t) - h]\} \quad Y^{IDR}(0) = 0 \end{aligned} \tag{10}$$

where secretory parameters and variables are labeled "idr" to indicate that they refer to insulin delivery rate and then account for secretion and hepatic extraction.

From model parameters, the IDR profile (pmol/min) was reconstructed as

$$IDR(t) = [nI_b + idr(t)]V_I = [nI_b + m^{IDR}X^{IDR}(t)]V_I \tag{11}$$

where I_b is the end-test insulin concentration.

Indexes of responsivity to glucose of first- and second-phase and basal insulin delivery rate were also calculated by using formulas similar to *Eqs. 6–8*:

$$\Phi_1^{IDR} = X_0^{IDR}/\Delta G \tag{12}$$

$$\Phi_2^{IDR} = \beta^{IDR} \tag{13}$$

$$\Phi_b^{IDR} = idr_b/G_b = nI_b/G_b \tag{14}$$

where G_b is the end-test glucose concentration.

Hepatic insulin extraction. From ISR and IDR profiles, the HE profile was reconstructed as

$$HE(t) = \frac{ISR(t) - IDR(t)}{ISR(t)} = 1 - \frac{IDR(t)}{ISR(t)} \tag{15}$$

From ISR and IDR indexes, two HE indexes, i.e., during IVGTT and in the basal state, were estimated as

$$HE = \frac{\int_0^T ISR(t)dt - \int_0^T IDR(t)dt}{\int_0^T ISR(t)dt} = 1 - \frac{(\Phi_b^{IDR} + \Phi_1^{IDR}A_1 + \Phi_2^{IDR}A_2)V_I}{(\Phi_b + \Phi_1 A_1 + \Phi_2 A_2)V_C}$$

$$HE_b = \frac{isr_b \cdot V_C - idr_b \cdot V_I}{isr_b \cdot V_C} = 1 - \frac{\Phi_b^{idr} V_I}{\Phi_b V_C} \tag{16}$$

$$A_1 = \frac{\Delta G}{T \cdot G_b} \quad A_2 = \frac{\int_0^T [G(t) - h]dt}{T \cdot G_b} \tag{17}$$

where T is the time at which glucose, insulin, and C-peptide concentrations reach their end-test values after the IVGTT perturbation.

Model identification. Identification of the two models was performed simultaneously in each subject by using SAAM II software (1), with the constraint that the threshold, h, assumes the same value in both models. Secretion parameters m, α, β, and X_0 were estimated from plasma C-peptide, and glucose data with C-peptide kinetic parameters were fixed to standard population values, following the method proposed by Van Cauter et al. (23), whereas insulin kinetic (n and V_I) and delivery rate parameters (m^{IDR}, α^{IDR}, β^{IDR}, $X_0{}^{IDR}$) were estimated from plasma insulin and glucose data.

Errors in insulin and C-peptide measurements were assumed to be uncorrelated, Gaussian, zero mean with a variance linked to insulin (I), and C-peptide (C) measurements according to the models, $Var(I) = 6 + 0.0055 \times I^2$ and $Var(C) = 2000 + 0.001 \times C^2$. The coefficients of variations (CVs) of insulin measurements then ranged from ~13% at basal level down to 8% (16) and that of C-peptide from 11% down to 4%.

Statistical analysis. Data are presented as means ± SD. Pearson's correlation coefficient was used to evaluate univariate correlation.

RESULTS

Average glucose, insulin, and C-peptide concentrations are shown in Fig. 3. A steady-state condition was reached at the end of the experiment at levels (4.58 ± 0.24 mmol/l, 18.3 ± 6.3 pmol/l, and 403 ± 114 pmol/l, respectively) somewhat lower than the pretest levels (5 ± 0.33 mmol/l, 25.3 ± 6.5 pmol/l, and 471 ± 121 pmol/l, respectively).

The ability of C-peptide and insulin minimal models to describe the data is shown in Fig. 4, where average weighted residuals are shown.

Estimated secretion parameters m, α, β, X_0, and h and indexes Φ_b, Φ_1, and Φ_2 are shown in Table 1. Estimated insulin kinetic parameters n and V_I, delivery rate parameters m^{IDR}, α^{IDR}, β^{IDR}, and $X_0{}^{IDR}$, and indexes $\Phi_b{}^{IDR}$, $\Phi_1{}^{IDR}$, and $\Phi_2{}^{IDR}$ in all individuals are summarized in Table 2.

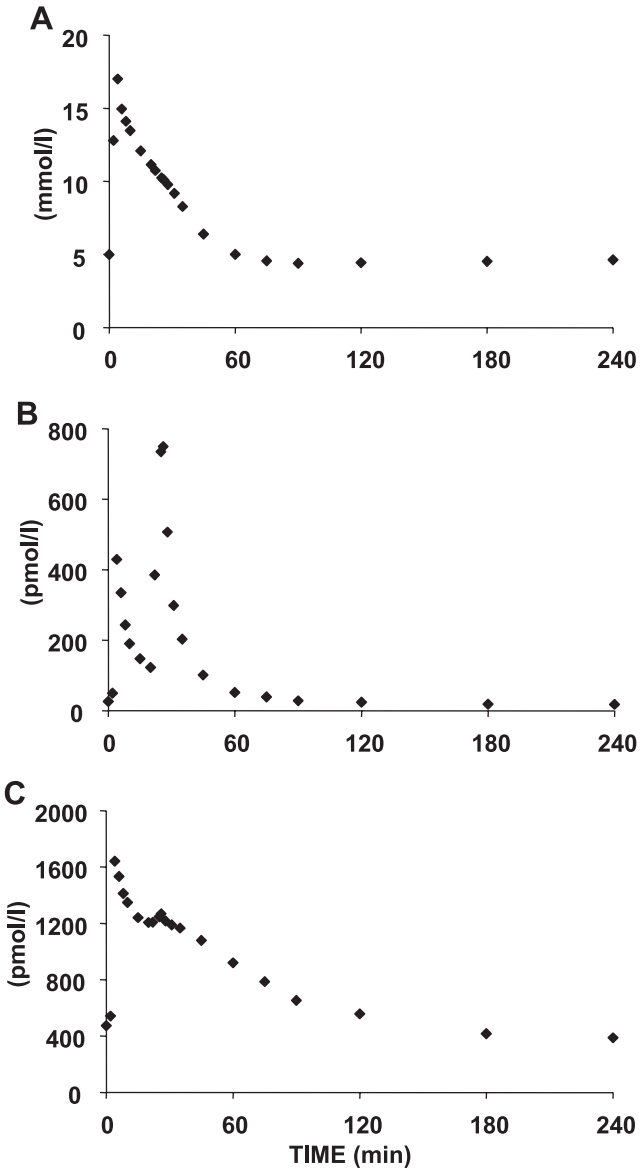

Fig. 3. Plasma glucose (*A*), insulin (*B*), and C-peptide (*C*) concentration during an IM-IVGTT (mean values in 20 normal subjects).

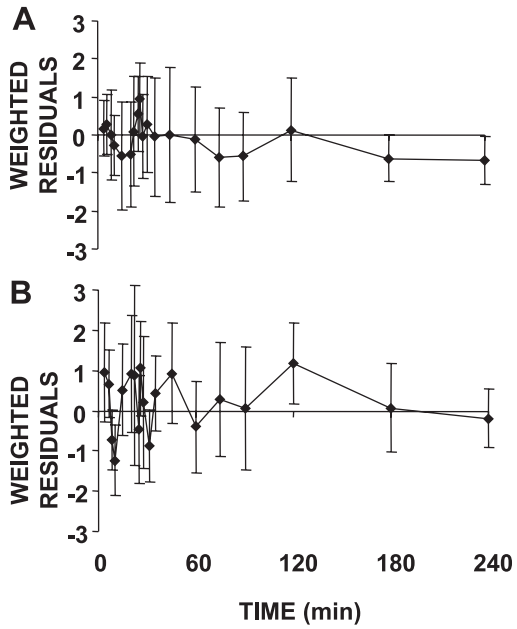

Fig. 4. Weighted residuals (means ± SD in 20 normal subjects) of C-peptide (*A*) and insulin (*B*) minimal models.

Parameter *h* was, on average, 4.6 ± 0.3 mmol/l, not significantly different from the end-test value of glucose concentration.

The minimal model-derived average HE profile is shown in Fig. 5. Starting from a pretest value of 64 ± 12%, HE is rapidly suppressed after the glucose bolus and then slowly reaches, within 120 min, a steady-state value HE_b of 70 ± 9%. Individual values of HE_b and HE indexes are shown in Table 3 and indicate that ~50% of secreted insulin is extracted by the liver during an IM-IVGTT.

DISCUSSION

The minimal-modeling approach, originally proposed to assess ISR during an IVGTT on the basis of C-peptide and glucose data, has been applied here to quantify IDR from insulin data, thus making it possible to noninvasively assess HE. The adopted model uses a functional description of the control of glucose on IDR similar to that proposed by us (20) for ISR. The model also includes a description of insulin kinetics to link secretion to insulin measurements taken in plasma. To reliably assess insulin kinetics, a prerequisite to avoid undesired compensations between parameters describing secretion and kinetics (20), the insulin minimal model was identified on IM-IVGTT data. This protocol associates the glucose bolus with a short insulin infusion 20 min after the bolus and was originally proposed to improve the identification of the glucose minimal model (9, 25). It also offers definite advantages for the identification of the insulin minimal model, because insulin decay data, measured after the insulin infusion, allowed a reliable estimation of insulin disappearance rate constant and distribution volume and, thus, of insulin clearance rate in each individual. Secretory parameters were estimated as well, thus allowing us to reconstruct the posthepatic secretion profile as well as derive indexes of first- and second-phase posthepatic secretion.

The combined use of insulin and C-peptide minimal models identified in the same subject provided quantitative information on the ability of the liver to extract insulin during any passage through it, because it enabled reconstruction of HE profile and calculation of two indexes that were able to quantify this process both in the basal state and during the glucose perturbation.

Insulin kinetics. A variety of models have been used in the literature to describe insulin kinetics, with the number of compartments ranging from one to three. Moreover, it has been suggested that insulin clearance may vary during a glucose and/or insulin perturbation. This is invariably reported in the case of sustained perturbations such as, e.g., 3-h hyperglycemic glucose clamp in humans (19), 1-h insulin infusion in dogs (15), and 42-h low-rate glucose infusion in humans (4). In the case of transient perturbations, such as those induced by an IM-IVGTT, it is generally acknowledged that insulin kinetics can be considered linear until insulin levels of 100–150 μU/ml (i.e., 600–900 pmol/l) are reached (5, 10, 12, 15). In the present study, a linear single-compartment model was assumed to describe insulin kinetics. The linearity assumption appears reasonable because insulin concentration remains within the linearity range for the largest part of the experiment. The monocompartmental assumption renders the whole model (secretion plus kinetics) uniquely a priori identifiable, which allowed us to estimate kinetic parameters with acceptable precision. Moreover, it provided a reasonable fit, particularly of data collected immediately after the exogenous insulin administration, and reliable estimates of kinetic parameters; e.g., insulin plasma clearance rate (PCR = $n \cdot V_I$) was 1.7 ± 0.36 (means ± SD) l/min, very similar to values reported by some authors (4, 17, 19). These findings confirm that the linear single-compartment model provides a reasonable description of insulin kinetics in situations like the present one. They also

Table 1. *Parameters and indexes of C-peptide model*

Subject	m, min^{-1}	α, min^{-1}	X_0, pmol/l	Φ_1, 10^{-9}	Φ_2, 10^{-9} min^{-1}	Φ_b, 10^{-9} min^{-1}
1	0.90 (71)*	0.17 (26)	2,429 (4)	182 (4)	10.1 (4)	6.8
2	0.75 (42)	0.13 (28)	1,766 (4)	147 (4)	6.7 (7)	2.8
3	0.43 (56)	0.05 (19)	1,094 (5)	72 (5)	6.7 (10)	4.8
4	0.87 (48)	0.05 (17)	2,589 (4)	173 (4)	7.6 (8)	7.6
5	0.61 (32)	0.07 (14)	1,093 (6)	55 (6)	7.8 (6)	4.2
6	0.56 (68)	0.05 (20)	556 (9)	41 (9)	5.8 (10)	4.7
7	0.39 (19)	0.11 (22)	2,101 (5)	156 (5)	7.7 (6)	5.9
8	0.66 (32)	0.10 (16)	1,251 (6)	83 (6)	10.0 (5)	8.0
9	0.61 (34)	0.19 (19)	1,085 (6)	84 (6)	11.2 (4)	5.0
10	0.34 (14)	0.02 (21)	1,870 (4)	193 (4)	13.5 (15)	4.5
11	0.16 (16)	0.13 (37)	2,518 (8)	305 (8)	6.9 (12)	5.7
12	0.64 (39)	0.19 (24)	2,067 (5)	184 (5)	10.7 (5)	5.2
13	0.71 (53)	0.13 (18)	1,321 (5)	106 (5)	9.7 (4)	5.8
14	0.92 (18)	0.12 (35)	1,119 (5)	65 (5)	4.5 (8)	4.6
15	0.77 (28)	0.18 (37)	1,372 (4)	161 (4)	6.5 (8)	3.8
16	0.78 (47)	0.16 (29)	1,991 (4)	168 (4)	7.2 (7)	6.1
17	1.13 (41)	0.17 (17)	4,302 (4)	277 (4)	15.1 (4)	7.2
18	0.70 (47)	0.27 (62)	1,440 (5)	126 (5)	4.5 (8)	2.8
19	0.76 (23)	0.16 (25)	2,724 (3)	205 (3)	3.3 (11)	2.9
20	0.53 (28)	0.36 (63)	2,563 (5)	260 (5)	9.5 (7)	5.3
Mean	0.66 (38)	0.14 (27)	1,863 (5)	152 (5)	8.2 (7)	5.2
SD	0.22	0.08	850	75	3.0	1.5

*Precision of parameter estimate expressed as %coefficient of variation. See text for definitions of parameters and indexes.

Table 2. *Parameters and indexes of insulin model*

Subject	n, min^{-1}	V_I, l	m^{IDR}, min^{-1}	α^{IDR}, min^{-1}	X_0^{IDR}, pmol/l	Φ_1^{IDR}, 10^{-9}	Φ_2^{IDR}, 10^{-9} min^{-1}	Φ_b^{IDR}, 10^{-9} min^{-1}
1	0.18 (8)*	9.7 (8)	0.51 (30)	0.16 (30)	912 (7)	68 (7)	2.9 (14)	0.73 (8)
2	0.27 (6)	6.8 (7)	1.11 (92)	0.08 (12)	875 (20)	73 (20)	3.2 (11)	0.52 (6)
3	0.12 (6)	13.1 (6)	0.59 (28)	0.01 (38)	382 (6)	25 (6)	0.9 (22)	0.42 (6)
4	0.14 (8)	11.2 (6)	0.88 (26)	0.06 (20)	834 (8)	56 (8)	1.7 (19)	0.92 (8)
5	0.21 (5)	8.5 (6)	0.83 (27)	0.05 (12)	230 (8)	12 (8)	1.5 (11)	0.41 (5)
6	0.19 (7)	9.8 (7)	0.78 (28)	0.04 (12)	243 (8)	18 (8)	2.5 (11)	0.68 (7)
7	0.21 (8)	9.3 (9)	1.02 (85)	0.15 (21)	1060 (14)	79 (14)	2.5 (13)	0.62 (8)
8	0.25 (9)	6.5 (12)	0.84 (27)	0.08 (11)	484 (11)	32 (11)	4.0 (13)	1.33 (9)
9	0.19 (8)	7.9 (8)	0.17 (30)	0.17 (21)	281 (16)	22 (16)	1.9 (20)	0.66 (8)
10	0.18 (7)	7.6 (9)	0.66 (31)	0.02 (23)	538 (7)	55 (7)	3.1 (15)	0.63 (7)
11	0.17 (11)	9.1 (11)	0.31 (24)	0.29 (65)	585 (10)	71 (10)	1.7 (28)	1.16 (11)
12	0.16 (8)	12.0 (6)	0.70 (25)	0.03 (16)	467 (7)	42 (7)	1.9 (16)	0.59 (8)
13	0.20 (8)	9.4 (8)	0.81 (27)	0.08 (11)	505 (9)	40 (9)	3.0 (13)	1.09 (8)
14	0.32 (7)	6.3 (8)	0.68 (18)	0.14 (17)	663 (8)	38 (8)	3.4 (12)	1.18 (7)
15	0.15 (7)	8.6 (7)	0.24 (13)	0.01 (42)	609 (7)	71 (7)	1.9 (27)	0.47 (7)
16	0.24 (7)	5.4 (8)	0.49 (19)	0.11 (16)	1167 (7)	98 (7)	2.4 (18)	0.90 (7)
17	0.10 (8)	9.6 (7)	0.85 (27)	0.03 (31)	1117 (6)	72 (6)	0.7 (36)	0.64 (8)
18	0.21 (8)	11.7 (8)	0.68 (34)	0.14 (18)	708 (8)	62 (8)	2.1 (19)	0.63 (8)
19	0.18 (6)	7.9 (6)	0.35 (13)	0.05 (18)	1449 (6)	109 (6)	1.4 (24)	0.66 (6)
20	0.18 (9)	13.1 (8)	0.27 (13)	0.06 (22)	921 (8)	93 (8)	1.5 (25)	0.66 (9)
Mean	0.19 (8)	9.2 (8)	0.64 (31)	0.09 (23)	701 (9)	57 (9)	2.2 (18)	0.74 (8)
SD	0.05	2.2	0.27	0.07	334	28	0.9	0.26

*Precision of parameter estimate expressed as % coefficient of variation. See text for definitions of parameters and indexes; IDR, insulin delivery rate.

support the validity of the minimal-model description of IDR, because we showed (20) that a reliable description of kinetic processes avoids errors in modeling the secretory processes.

IDR. The model adopts a functional description of the control of glucose on IDR similar to that used in the C-peptide minimal model (20). Parameters and indexes estimated from insulin data (Table 2) assumed values that were different from their counterparts estimated from C-peptide data (Table 1), because they also accounted for HE. Only the threshold of glucose concentration that is able to stimulate ISR and IDR is forced to be the same. The estimated value is very close to the constant level reached by glucose at the end of the experiment, when insulin and C-peptide concentrations are almost constant. These concentrations were adopted as the basal concentrations to allow the two models to reach a steady-state condition at the end of the experiment. The basal responsivity to glucose Φ_b^{IDR} was $0.74 \pm 0.26 \cdot 10^{-9} \cdot min^{-1}$, representing 15% as an average of its pancreatic counterpart. By multiplying responsivities, which are related to secretion per unit of distribution volume, by insulin and C-peptide distribution volumes 9.17 and 4.5 l, respectively, basal responsivity accounted for 30% of pancreatic responsivity and correlated well with it ($R = 0.53$).

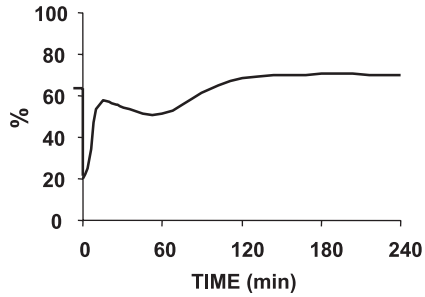

Fig. 5. Hepatic extraction during an insulin-modified intravenous glucose tolerance test (mean in 20 normal subjects).

First- and second-phase responsivity to glucose were $57 \pm 28 \cdot 10^{-9} \cdot min^{-1}$ and $2.2 \pm 0.9 \cdot 10^{-9} \cdot min^{-1}$, accounting for 39 and 30%, respectively (77 and 59%, respectively, after volume correction), of their pancreatic counterparts.

HE. HE was assessed by combining the information derived from the two minimal models. The HE profile showed a rapid suppression immediately after the glucose bolus administration, followed by a rapid increase that was attenuated at 20 min, when insulin was administered (Fig. 5). Then, it returned to steady state at the end of the experiment at a value (70 ± 9%) different from the pretest value (64 ± 12%), which was

Table 3. *Indexes of hepatic extraction*

Subject	HE_b, %	HE, %
1	77 (2)*	57 (5)
2	70 (2)	46 (12)
3	76 (1)	63 (3)
4	72 (2)	58 (6)
5	81 (1)	73 (2)
6	69 (2)	47 (7)
7	80 (1)	55 (7)
8	75 (2)	61 (5)
9	77 (2)	72 (3)
10	76 (1)	67 (3)
11	59 (4)	56 (6)
12	69 (2)	59 (4)
13	63 (3)	52 (6)
14	59 (3)	35 (11)
15	72 (2)	52 (5)
16	79 (1)	63 (4)
17	80 (1)	72 (3)
18	46 (6)	19 (32)
19	60 (3)	36 (10)
20	65 (3)	46 (8)
Mean	70 (2)	54 (7)
SD	9	14

*Precision of parameter estimate expressed as %coefficient of variation. HE, hepatic extraction.

expected because insulin and C-peptide data are different in the two situations. These results indicate that HE varies in time during a transient glucose perturbation. They are consistent with previous observations, obtained, e.g., in dogs by using invasive methods (13) or in humans by using a modeling approach similar to the one adopted here (6). However, in evaluating the model-predicted pattern of HE, it is important to consider that its ingredients, the model-predicted ISR and IDR, are in fact the rate of appearance in plasma of C-peptide molecules resulting from secretion and transit through the liver and of newly secreted insulin molecules resulting from secretion, HE, and transit through the liver, respectively. However, the liver not only degrades a fraction of insulin molecules but also introduces a delay; e.g., for insulin, a transit time equal to 43 s in humans (8) and 2 min in dogs (7) was reported. Should the transit time of C-peptide be different than that of insulin, the HE profile shown in Fig. 5 accounts not only for the time course of HE but also for differences in the way the liver handles insulin and C-peptide molecules. By contrast, these differences do not affect HE indexes: HE_b is calculated in steady-state conditions, i.e., in a situation where inward and outward hepatic fluxes are equal, whereas HE (*Eq. 10*) is defined from IDR and ISR integrals that are not affected by the liver delay. Our results (Table 3) indicate that the liver is able to extract 70 ± 9% of the insulin passing through it in the end-test basal state and 54 ± 14% during IM-IVGTT. A possible explanation is that liver saturation mechanisms are activated at insulin concentration levels observed during IM-IVGTT. In addition, one can also call for an increase in hepatic blood flow, induced by IM-IVGTT, which has been shown to be associated with a reduced HE (22). Our values are in good agreement with previous findings in the steady state, as reviewed by Ferrannini and Cobelli (8), and during an IVGTT perturbation (6).

Regarding HE estimation, our results indicate that HE_b and HE can be estimated with very good precision, i.e., with CVs respectively equal to 3 and 7%. CVs were calculated by propagating the precision of all model parameters included in HE_b and HE formulas (*Eqs. 15* and *16*). However, glucose data, as well as basal insulin and C-peptide levels, are assumed to be noise free, and C-peptide distribution volume V_C was fixed to a population value and adjusted according to the body surface area, following the method proposed by Van Cauter et al. (23). Because V_C plays a crucial role in HE_b and HE calculations, we evaluated through a sensitivity analysis that the average percentage sensitivities of HE_b and HE to percentage errors in V_C are 0.45 ± 0.23 and 1.02 ± 0.87, respectively. The order of magnitude of errors in V_C can be evaluated as 20% from a study on seven subjects for whom reference values were available (11). From the sensitivity analysis, they reflected a 10 and 20% increase in HE_b and HE precision, thus moving from 3 and 7% (Table 3) to still acceptable values of 13 and 27%, respectively.

HE and insulin clearance. HE is a component of insulin PCR, accounting for ~58% of the total flux (from the data reviewed in Ref. 8). Our data in fact indicate a significant correlation of PCR with both HE_b ($R = 0.48$, $P = 0.03$) and HE ($R = 0.60$, $P = 0.005$).

The reduction predicted by the two minimal models in HE during IM-IVGTT is apparently in contrast with the linearity assumption of insulin kinetics. However, the 23% reduction in HE estimated during an IM-IVGTT with respect to basal (from 70 to 54%; Table 3), although reflecting in a 23% reduction of the hepatic component of insulin clearance (from 0.58 PCR to 0.45 PCR), accounts only for a lower percentage decrease of insulin clearance (to 0.45 PCR + 0.42 PCR = 0.87 PCR) if nonhepatic insulin clearance is assumed to be linear during IM-IVGTT (thus remaining constant at 0.42 PCR). Because a 13% reduction of insulin clearance is hard to detect from our data, we can speculate that insulin clearance is likely to vary in time during an IM-IVGTT due to variations in HE, but these variations are modest and difficult to detect from plasma insulin data. Only a constant value of PCR can be estimated, which represents the overall clearance value during IM-IVGTT. To check the reliability of these assumptions, we have developed an alternative model that links insulin clearance to HE. The model, detailed in the APPENDIX, describes insulin clearance as the sum of two processes: hepatic clearance, varying in time with a pattern proportional to HE profile, and peripheral clearance, assumed to be constant. Numerical identification was successfully achieved only by fixing a priori the ratio between the two processes at basal state. This is a critical issue that is likely to vary among subjects/conditions. When a plausible value was used, e.g., at basal state, hepatic clearance accounted for 60% of the total clearance, the new model provided a fit similar to that of the original model (data not shown). However, values of basal insulin clearance were plausible in only 17 of our 20 subjects (in 3 subjects, implausibly high values of basal clearance of 5.8, 4.2, and 3.4 l/min were estimated, associated with elevated values of secretion indexes). In the remaining 17 subjects, the new model provided an average insulin clearance that was very similar and well correlated to that estimated with the original model (1.7 ± 0.5 vs. 1.6 ± 0.3 l/min, $R = 0.74$, $P = 0.001$). Overall, HE indexes were also very similar and well correlated to those derived from the original model (HE_b = 69 ± 9 vs. 72 ± 7%, $R = 0.71$, $P = 0.001$; HE = 57 ± 12 vs. 58 ± 10%, $R = 0.72$, $P < 0.001$), thus indicating that HE indexes of the original model are robust with respect to variations in insulin clearance observed during an IVGTT.

HE and C-peptide/insulin molar ratios. Finally, let us relate our HE indexes to C-peptide/insulin molar ratios, which are often used as indicators of hepatic insulin extraction. In Polonsky and Rubenstein (14), the use of the ratio between incremental areas under plasma C-peptide and insulin concentration curves as a reflection of HE was discussed, and it was pointed out that the marked difference in the plasma half-lives of insulin and C-peptide complicates the interpretation of changes in this ratio. By integrating *Eq. 9*, it is possible to link the incremental area under insulin concentration to the total amount of delivered insulin and to insulin clearance rate (nV_I)

$$\int_0^T I(t)dt = \frac{V_I \int_0^T idr(t)dt + \int_0^T U(t)dt}{n \cdot V_I} \qquad (18)$$

where the integral of the exogenous input U(t) is the administered insulin dose.

Similarly, by integrating *Eq. 1*, one has a relationship between the incremental area under C-peptide concentration, the total amount of secreted hormone, and C-peptide clearance rate ($k_{01}V_C$):

$$\int_0^T \mathrm{CP}_1(t)\mathrm{d}t = \frac{V_C \int_0^T \mathrm{isr}(t)\mathrm{d}t}{k_{01}V_C} \qquad (19)$$

During an IM-IVGTT, the ratio between incremental C-peptide and insulin areas (*Eqs. 18* and *19*) represents only a semiquantitative indicator of HE, because it also depends on the total amount of infused insulin and insulin and C-peptide clearance rates. Conversely, the minimal-model index HE (*Eq. 16*) represents a correct measure of HE in terms of the incremental areas of pancreatic and posthepatic secretion.

In conclusion, insulin secretion, kinetics, and hepatic extraction can be assessed by using the insulin and C-peptide minimal models on IM-IVGTT data. These models, used in conjunction with the minimal model of glucose kinetics (3), thus provide indexes such as insulin sensitivity, glucose effectiveness, first- and second-phase responsivity to glucose of insulin secretion, insulin clearance, and hepatic extraction, which represent a rich parametric picture of the glucose-regulatory system that is usable for studying pathophysiological states such as impaired glucose tolerance, obesity, and diabetes.

APPENDIX

To include in the model a link between insulin clearance and HE, insulin clearance was described as the sum of two processes: hepatic clearance, varying in time with a pattern proportional to hepatic extraction; and peripheral clearance, which was assumed to be constant. Thus the equation describing insulin kinetics is

$$\dot{\mathrm{I}}(t) = -[n^{\mathrm{H}}\mathrm{HE}(t) + n^{\mathrm{P}}]\mathrm{I}(t) + \mathrm{idr}(t) + \mathrm{U}(t)/V_{\mathrm{I}} \quad \mathrm{I}(0) = 0 \qquad (A1)$$

where n^{H} HE(t) (min^{-1}) represents hepatic clearance per unit distribution volume, modulated by HE, and n^{P} (min^{-1}) represents the contribution of peripheral clearance, which was assumed to be constant during the experiment.

For HE, *Eq. 15* was used

$$\dot{\mathrm{I}}(t) = -\left[n^{\mathrm{H}}\left(1 - \frac{\mathrm{IDR}(t)}{\mathrm{ISR}(t)}\right) + n^{\mathrm{P}}\right]\mathrm{I}(t) + \mathrm{idr}(t) + \mathrm{U}(t)/V_{\mathrm{I}} \quad \mathrm{I}(0) = 0 \qquad (A2)$$

where ISR is described by *Eq. 5*, whereas IDR now accounts for both hepatic and peripheral clearance:

$$\mathrm{IDR}(t) = [\mathrm{idr}_{\mathrm{b}} + \mathrm{idr}(t)]V_{\mathrm{I}} = [(n^{\mathrm{H}}\mathrm{HE}_{\mathrm{b}} + n^{\mathrm{P}})\mathrm{I}_{\mathrm{b}} + \mathrm{idr}(t)]V_{\mathrm{I}} \qquad (A3)$$

The new insulin model consists of *Eq. A2* coupled with *Eq. 10* to describe idr. It was simultaneously identified with the C-peptide model, *Eqs. 1–4*, which provides a description for ISR appearing in *Eq. A2*. To achieve numerical identification, a constraint was introduced on the relative contribution of hepatic and peripheral clearance in the basal state; namely, it was assumed that, in all subjects, hepatic and peripheral clearance account for 60 and 40%, respectively, of the basal clearance:

$$\frac{n^{\mathrm{H}}\mathrm{HE}_{\mathrm{b}}}{n^{\mathrm{P}}} = \frac{60}{40} \qquad (A4)$$

GRANTS

This study was partially supported by National Institutes of Health Grants DK-29953 and RR-00585 and by Ministero dell'Università e della Ricerca Scientifica, Italy

REFERENCES

1. **Barrett PH, Bell BM, Cobelli C, Golde H, Schumitzky A, Vicini P, and Foster DM.** SAAM II: simulation, analysis and modeling software for tracer and pharmacokinetics studies. *Metabolism* 47: 484–492, 1998.
2. **Basu R, Breda E, Oberg AL, Powell CC, Dalla Man C, Basu A, Vittone JL, Klee GG, Arora P, Jensen MD, Toffolo G, Cobelli C, and Rizza RA.** Mechanisms of the age-associated deterioration in glucose tolerance: contribution of alterations in insulin secretion, action, and clearance. *Diabetes* 52: 1738–1748, 2003.
3. **Bergman RN, Ider YZ, Bowden CR, and Cobelli C.** Quantitative estimation of insulin sensitivity. *Am J Physiol Endocrinol Metab Gastrointest Physiol* 236: E667–E677, 1979.
4. **Byrne MM, Sturis J, and Polonsky KS.** Insulin secretion and clearance during low-dose graded glucose infusion. *Am J Physiol Endocrinol Metab* 268: E21–E27, 1995.
5. **Cobelli C, Mari A, and Ferrannini E.** On linearity of insulin kinetics. *Am J Physiol Endocrinol Metab* 251: E247–E250, 1986.
6. **Cobelli C and Pacini G.** Insulin secretion and hepatic extraction in humans by minimal modeling of C-peptide and insulin data. *Diabetes* 37: 223–231, 1988.
7. **Eaton RP, Allen RC, Schade DS, Erickson KM, and Standefer J.** Prehepatic insulin production in man: kinetic analysis using peripheral connecting peptide behaviour. *J Clin Endocrinol Metab* 51: 520–528, 1980.
8. **Ferrannini E and Cobelli C.** The kinetics of insulin in man. II. Role of the liver. *Diabetes Metab Rev* 3: 365–397, 1987.
9. **Finegood DT, Hramiak IM, and Dupre J.** A modified protocol for estimation of insulin sensitivity with the minimal model of glucose kinetics in patients with insulin dependent diabetes. *J Clin Endocrinol Metab* 70: 1538–1549, 1990.
10. **Hovorka R, Poeriw JK, Smith GD, Sucharda P, and Sonka J.** Five-compartment model of insulin kinetics and its use to investigate action of chloroquine in NIDDM. *Am J Physiol Endocrinol Metab* 265: E162–E175, 1993.
11. **Magni P, Bellazzi R, Sparacino G, and Cobelli C.** Bayesian identification of a population compartmental model of C-peptide kinetics. *Ann Biomed Eng* 28: 812–823, 2000.
12. **Morishima T, Bradshaw C, and Radziuk J.** Measurement using tracers of steady-state turnover and metabolic clearance of insulin in dogs. *Am J Physiol Endocrinol Metab* 248: E203–E208, 1985.
13. **Morishima T, Pye S, Bradshaw C, and Radziuk J.** Posthepatic rate of appearance of insulin: measurement and validation in the nonsteady state. *Am J Physiol Endocrinol Metab* 263: E772–E779, 1992.
14. **Polonsky KS and Rubenstein AH.** C-peptide as a measure of the secretion and hepatic extraction of insulin. Pitfalls and limitations. *Diabetes* 33: 486–494, 1984.
15. **Pye S, Wattarai T, Davies G, and Radziuk J.** Comparison of the continuously calculated fractional splanchnic extraction of insulin with its fractional disappearance using a new double tracer technique. *Metabolism* 42: 145–153, 1993.
16. **Robbins DC, Andersen L, Bowsher R, Chance R, Dinesen B, Frank B, Gingerich R, Goldstein D, Widemeyer HM, Haffner S, Hales CN, Jarett L, Polonsky K, Porte D, Skyler J, Webb G, and Gallagher K** Report of the American Diabetes Association's task force on standardization of the insulin assay. *Diabetes* 45: 242–256, 1996.
17. **Shapiro ET, Tillil H, Rubenstein AH, and Polonsky KS.** Peripheral insulin parallels changes in insulin secretion more closely than C-peptide after bolus intravenous glucose administration. *J Clin Endocrinol Metab* 67: 1094–1099, 1988.
18. **Tillil H, Shapiro ET, Miller MA, Karrison T, Frank BH, Galloway GA, Rubenstein AH, and Polonsky KS.** Dose-dependent effects of oral and intravenous glucose on insulin secretion and clearance in normal humans. *Am J Physiol Endocrinol Metab* 254: E349–E357, 1988.
19. **Tillil H, Shapiro T, Rubenstein AH, Galloway JA, and Polonsky KS.** Reduction of insulin clearance during hyperglycemic clamp. Dose-response study in normal humans. *Diabetes* 37: 1351–1357, 1988.

20. **Toffolo G, De Grandi F, and Cobelli C.** Estimation of beta-cell sensitivity from IVGTT C-peptide data. Knowledge of the kinetics avoids errors in modeling the secretion. *Diabetes* 44: 845–854, 1995.
21. **Toffolo G, Cefalu W, and Cobelli C.** Beta-cell function during insulin modified IVGTT successfully assessed by the C-peptide minimal model. *Metabolism* 48: 1162–1166, 1999.
22. **Tura A, Ludvik B, Nolan JJ, Pacini G, and Thomaseth K.** Insulin and C-peptide secretion and kinetics in humans: direct and model-based measurements during OGTT. *Am J Physiol Endocrinol Metab* 281: E966–E974, 2001.
23. **Van Cauter E, Mestrez F, Sturie J, and Polonsky KS.** Estimation of insulin secretion rates from C-peptide levels. Comparison of individual and standard kinetic parameters for C-peptide clearance. *Diabetes* 41: 368–377, 1992.
24. **Volund A, Polonsky KS, and Bergman RN.** Calculated pattern of intraportal insulin appearance without independent assessment of C-peptide kinetics. *Diabetes* 36: 1195–1202, 1987.
25. **Welch S, Gebhart SS, Bergman RN, and Phillips LS.** Minimal modeling analysis of intravenous glucose tolerance test-derived insulin sensitivity in diabetic subjects. *J Clin Endocrinol Metab* 71: 1508–1518, 1990.